camera (Olympus Corporation, Tokyo, Japan). The width of the scratch wounds (ratio of migrated cells) was measured using NIH Image J software. As previously reported [41], the relative fold-change of the scratch wound width (%) at 10 h after introduction of the scratch wound compared with the control was calculated as the average of at least three fields (10 h scratched area/0 h scratched area after introduction of the scratch wound compared with new growth.

Invasion assay

An invasion assay was performed as previously described [42]. Cell invasion was measured using BD Matrigel (BD Bioscience, Franklin Lakes, NJ, USA) according to the manufacturer instructions. Briefly, 5×10^5 cells in 2 mL of serum-free medium were seeded into the upper chamber of the system (8 μm pore, 6-well format). The bottom wells in the system were filled with DMEM with 10% FBS as a chemoattractant. After incubation (143B: 12 h, HS-Os-1 and GLI2ΔN/YKNK12: 24 h), the cells in the upper chamber were removed, and the cells outside of the bottom membrane were stained with Hoechst 33342 (Life Technologies). Cells that had invaded through Matrigel were counted in five random fields of the membrane. The invasion efficiency of the control cells was defined as 100%.

DNA microarray analysis

Total RNA that had been extracted from U2OS cells treated with control siRNA or GLI2 siRNA (48 h) was examined to analyze the gene expression profiles of the cells. We used the Human Gene 1.0 ST Array (Affymetrix, Inc, Santa Clara, CA, USA). GeneChip microarray was performed by Bio Matrix Research, Inc (Chiba, Japan). Genes with more than 1.5-fold up- or down-regulation GLI2 siRNA-treated U2OS cells were identified using GeneSpring GX11 software (Agilent technologies). The data were deposited in the NCBI GEO database with the accession number GSE42903.

Kaplan–Meier analysis

The cutoff value that was used to determine the high expression level of RPS3 was determined using ROC analysis, and was calculated at 65.9%. Kaplan–Meier analysis was estimated in patients with RPS3 high- or low-expression levels.

Statistical analysis

All data are expressed as mean ± SD. Statistical analyses were performed using Student's *t*-tests, Mann–Whitney's U tests, and log-rank tests in Microsoft Office Excel and Prism. ROC and Kaplan–Meier analyses were performed using Excel Statistics 2012 (SSRI, Tokyo, Japan). *P* values less than 0.05 were considered significant.

Results

RPS3 *is a novel downstream gene of GLI2*

We previously reported that the Hedgehog pathway is activated in osteosarcoma cells. Furthermore, expression of *GLI2* was significantly upregulated in human osteosarcoma cell lines and specimens [20,39]. In addition, knockdown of *GLI2* decreased osteosarcoma cell invasion and lung metastases [22]. To gain further insight into the molecular mechanisms underlying GLI2-mediated migration and invasion of osteosarcoma, we performed a microarray analysis. We observed that 104 genes were downregulated (>1.5-fold) in *GLI2* RNAi-treated osteosarcoma cells (Appendix: Supplementary Fig. S1B). Among these, we selected several genes that were reported to regulate the proliferation and metastasis of cancer cells. We analyzed the expression of RPS3 proteins on invasive osteosarcoma cell lines (143B, U2OS, HOS, and HS-Os-1) and non-invasive osteosarcoma cell lines (Saos-2, MG63, and HuO9) [43,44]. The expression of RPS3 tended to increase protein in invasive osteosarcoma cells compared with non-invasive osteosarcoma cells (Fig. 1A). Knockdown of *GLI2* in 143B and Hs-Os-1 cells decreased the expression levels of RPS3 (Fig. 1B). A constitutively active form of GLI2 (GLI2ΔN) increased the expression of *RPS3* mRNA in YKNK-12 cells (Fig. 1C). Additionally, real-time PCR showed that transcription of *GLI2*, *PTCH1*, and *RPS3* mRNA was significantly increased by stimulation of rSHH (Fig. 1D). We previously reported that treatment with the FDA-approved drug arsenic trioxide (ATO) inhibited the invasion and metastasis of osteosarcoma cells through reduction of *GLI* transcription [19,22]. Expression of *RPS3* mRNA in osteosarcoma cells was decreased by ATO treatment (Fig. 1E). We also identified several GLI-binding sites within the *RPS3* promoter (Fig. 1F). These findings suggest that GLI promoted the expression of *RPS3*.

RPS3 regulates the migration and invasion of osteosarcoma cells

We examined the function of RPS3 in the migration and invasion of osteosarcoma cells. 143B and HS-Os-1 were treated with *RPS3* siRNA, which decreased the expression of RPS3 protein (Fig. 2A). Knockdown of *RPS3* significantly inhibited migration and invasion in osteosarcoma cell lines (Fig. 2A). We previously reported that forced expression of GLI2ΔN increased the migration of YKNK-12 human mesenchymal stem cell (GLI2ΔN/YKNK-12) [22]. We used GLI2ΔN/YKNK-12 to evaluate the role of RPS3 in migration and invasion of osteosarcoma. Migration and invasion of GLI2ΔN/YKNK-12 cells were greater than those of control vector-transfected YKNK-12 cells (control/YKNK-12), and knockdown of *RPS3* in control/YKNK-12 cells did not affect migration and invasion. However, the upregulated phenotypes of GLI2ΔN/YKNK-12 cells were decreased by knockdown of *RPS3* (Fig. 2B). We also found that forced expression of RPS3 increased the migration and invasion of shcontrol/143B cells (Vector shcontrol/143B vs. RPS3 shcontrol/143B). The reduction in migration and invasion by *GLI2* knockdown was recovered by forced expression of RPS3 (Fig. 2C). These findings suggest that the *RPS3* gene is downstream of GLI2 and mediates migration and invasion of osteosarcoma cells.

RPS3 expression in osteosarcoma tissue was higher in patients with lung metastasis

Immunohistochemical examination showed that the expression of RPS3 was higher in osteosarcoma tissue compared with that in normal bone. Less than 2% of cells in normal bone were weakly stained; thus, this was regarded as negative because the staining was too weak and the staining pattern was clearly different from that of positively-stained osteosarcoma cells (Fig. 3A). The number of RPS3-positive cells in osteosarcoma tissue was significantly increased in patients with lung metastasis (Fig. 3B). Statistically significant differences could not be achieved because of the small number of patients, and patients with high RPS3 expression showed relatively shorter survival times (Appendix: Supplementary Fig. S1C). Additionally, RPS3 expression level was high in tissue in which GLI2 expression level was high, such as cases #2, #4, and #5 (Table 1). Our findings suggest that RPS3 might be a marker of highly invasive osteosarcoma.

Discussion

It has been reported that aberrant activation of the Hedgehog pathway can drive tumorigenesis. Recent studies showed that GLI activation is involved in the progression of osteosarcoma [19,44,45]. We previously demonstrated that knockdown of GLI2 inhibited proliferation of osteosarcoma cells through regulation of the cell cycle, and inhibited the growth of osteosarcoma *in vivo* [20]. In addition, inhibition of GLI2 prevents osteosarcoma invasion and lung metastases [22]. Additionally, it was reported that the Smad- and GLI-mediated signaling pathways are activated in high-grade conventional osteosarcoma [46]. To identify the downstream gene of GLI2, we performed a microarray analysis. Consequently, we selected several genes as novel downstream genes of GLI2, including *RPS3, CLNS1A, LIPH, TFPI, MMP3, PSG4, FLAP, OLAH*, and *MILR1*. No significant association with GLI2 expression was found, and with the exception of *RPS3*, knockdown of these genes did not inhibit the migration of osteosarcoma cells (Appendix: Supplementary Fig. S1D); knockdown of *RPS3* markedly decreased the migration and

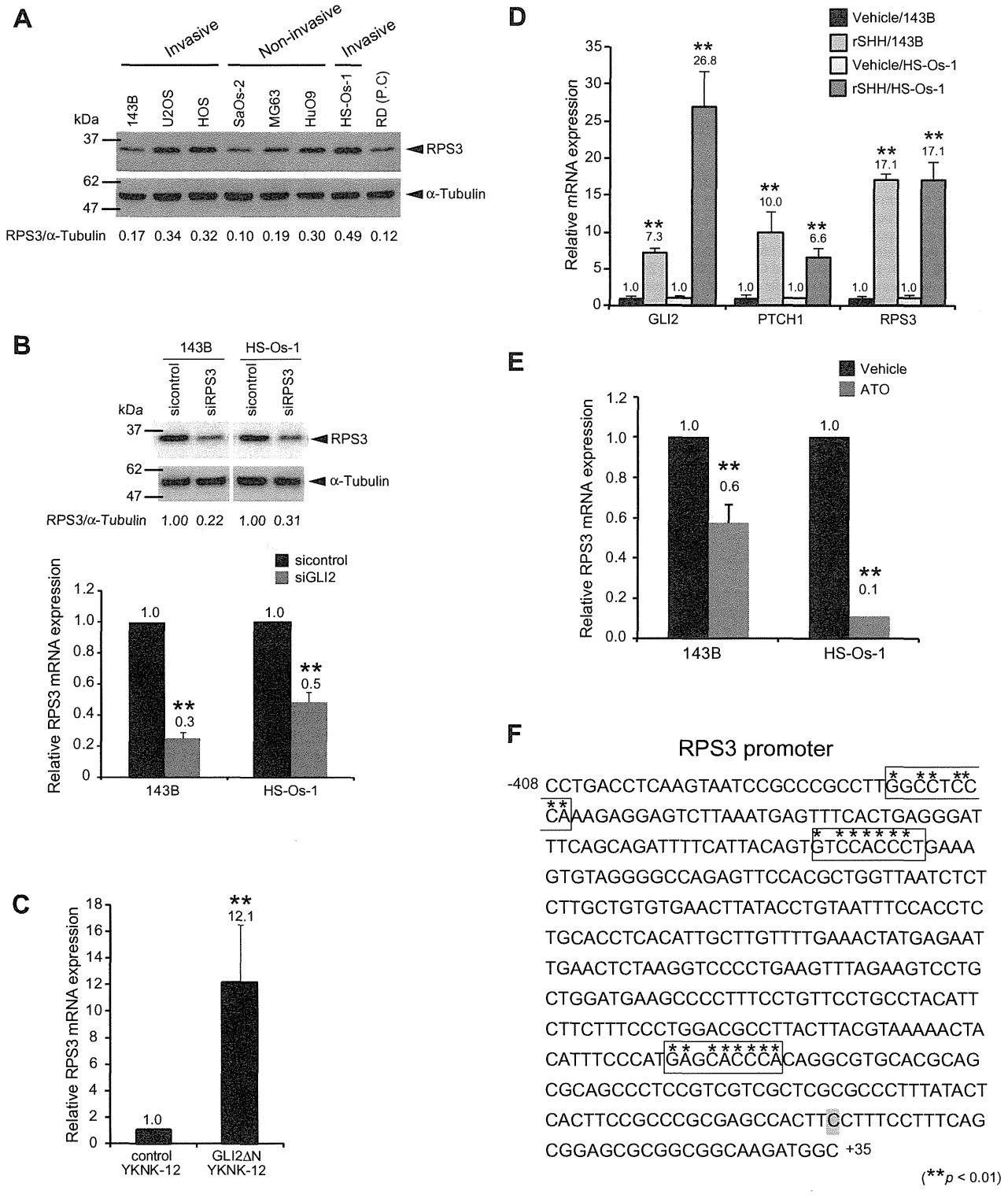

Fig. 1. GLI2 regulates *RPS3* expression. (A) The expression of RPS3 protein in invasive osteosarcoma cell lines (143B, U2OS, HOS, and HS-Os-1) and non-invasive osteosarcoma cell lines (Saos-2, MG63, and HuO9) were assessed using western blotting. Comparisons were made with NHOST cells, which were defined as 1.0. (B and C) After 72 h of RNAi treatment, *RPS3* mRNA levels in *GLI2* siRNA/143B or HS-Os-1, and stable GLI2ΔN/YKNK-12 cell lines were examined using real-time PCR and western blotting. Comparisons were made with control siRNA- or control vector-transfected cells, for which the relative expression was defined as 1.0. (D) Expression of *GLI2*, *PTCH1*, and *RPS3* mRNA in 143B or HS-Os-1 cells was assessed using real-time PCR following treatment with 500 ng/mL of rSHH for 48 h. Comparisons were made with vehicle-treated cells, for which the relative expression was defined as 1.0. (E) After 24 h treatment with 0.5 μM ATO, *RPS3* mRNA levels in vehicle- or ATO-treated 143B and HS-OS-1 cell lines were examined using real-time PCR. Comparisons were made with vehicle-transfected cells, for which the relative expression was defined as 1.0. (F) Genomic DNA sequences of *RPS3* promoters. Gray boxes indicate the transcription initiation point. Normal boxes indicate GLI-binding sites; GACCACCCA and asterisks show matched genes. $^{**}P < 0.01$, one-way ANOVA (A) and Student's *t*-tests (B–E).

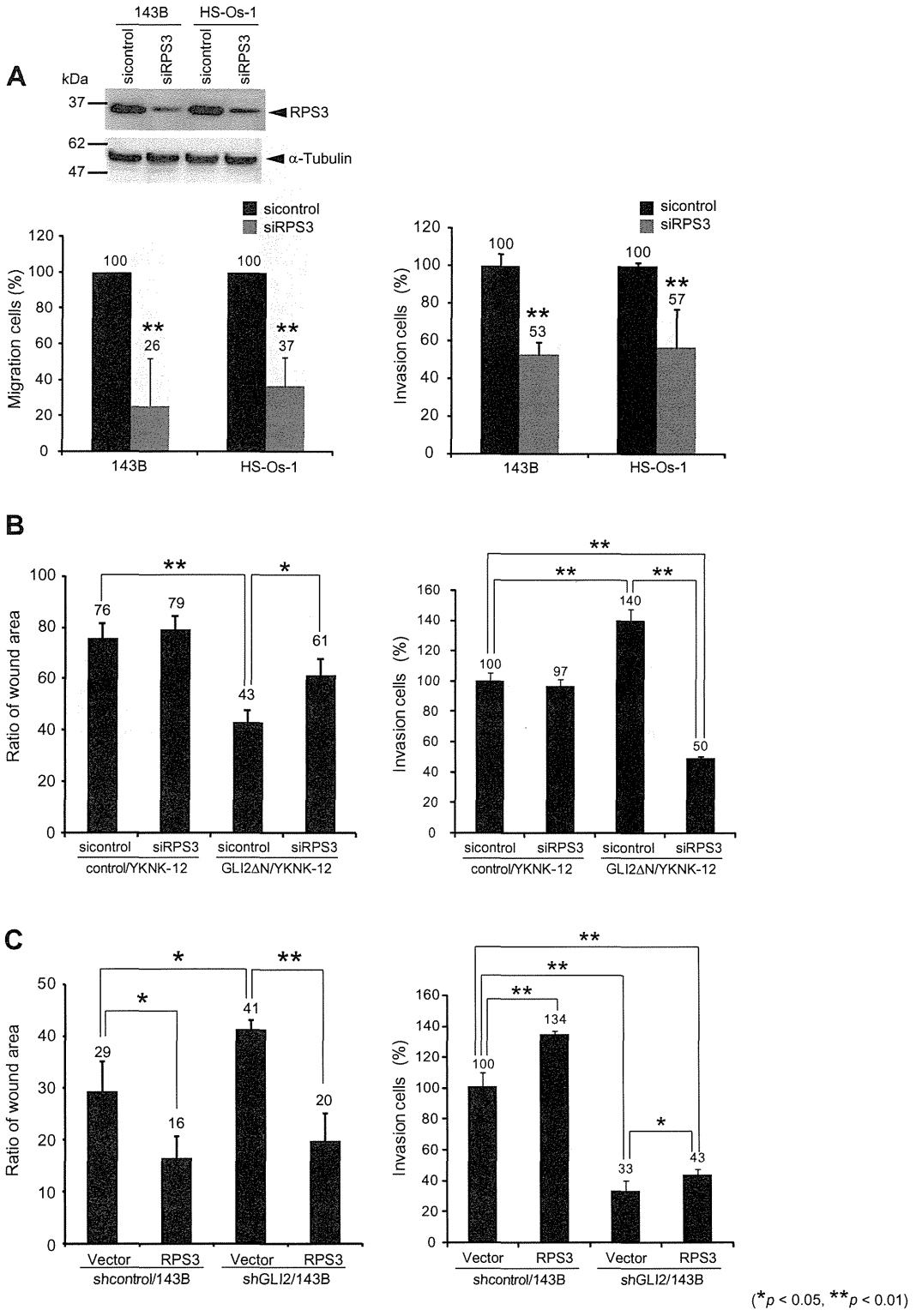

Fig. 2. RPS3 is a novel downstream factor of GLI2 that promotes invasiveness of osteosarcoma cells. (A) After 48 h treatment with RNAi, RPS3 protein levels in 143B and HS-Os-1 cells that were transfected with control siRNA (sicontrol) or *RPS3* siRNA (siRPS3) were examined using western blotting. After 24 h treatment with RNAi, migrated *RPS3* siRNA-143B or -HS-Os-1 cells were examined using wound healing assays. Invading cells were examined using an invasion assay. The percentage of migrating or invading cells in control siRNA-transfected cell lines was defined as 1 or 100% (bottom). (B) After 24 h treatment with RNAi, *RPS3* siRNA-treated control/YKNK-12 or GLI2A-treated migrated or invaded cells were examined using wound healing or invasion assays. The wound area ratio was calculated. Invading cells (%) in control siRNA-transfected control/YKNK-12 cells were defined as 100. (C) After 24 h of transfection with overexpression vector, migrating or invading control vector- (Vector) or RPS3 expression vector (RPS3)-transfected control shRNA/143B (shcontrol) or *GLI2* shRNA/143B (shGLI2) cells were examined using wound healing or invasion assays. The wound area ratio was calculated. Invading cells (%) in control siRNA-transfected control/YKNK-12 cells were defined as 100. $^{*}P < 0.05$ $^{**}P < 0.01$, Student's *t*-tests (A) and one-way ANOVA (B and C).

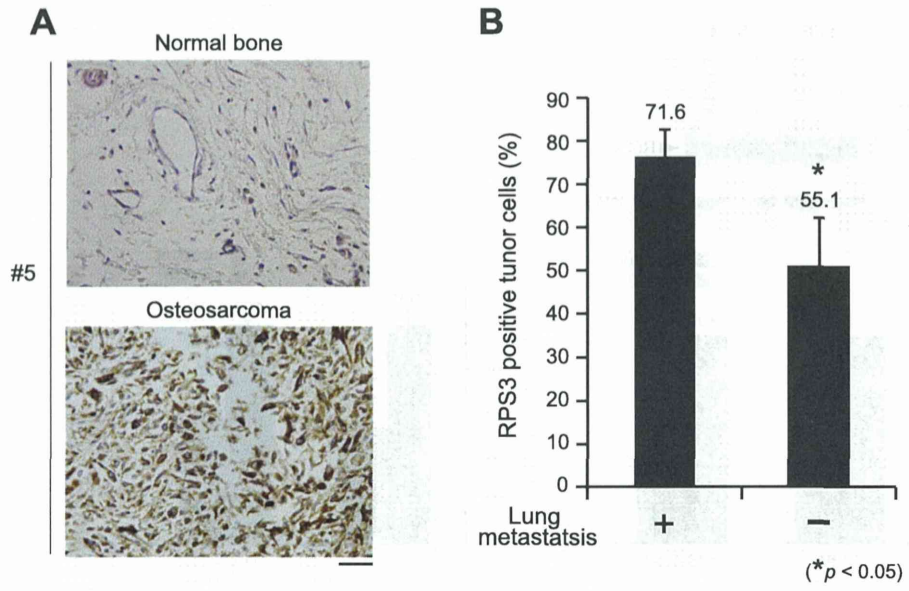

Fig. 3. RPS3 expression is high in osteosarcoma patient tissues. (A) Immunohistochemical staining of RPS3 was conducted in nine patients with osteosarcoma. Staining was also conducted in adjacent normal bone tissues for these patients. Expression of RPS3 was observed in osteosarcoma tissues (#5), but was not seen in normal bone tissues. The scale bar indicates 100 μm. (B) RPS3-positive cells in osteosarcomas with lung metastasis ($n = 3$) or without lung metastasis ($n = 6$) were calculated using data from Table 1. *$P < 0.05$, Mann–Whitney's U tests.

invasion of osteosarcoma cells. In contrast, forced expression of RPS3 promotes the migration and invasion of osteosarcoma cells. These findings suggest that RPS3 mediates the migration and invasion of osteosarcoma cells.

Knockdown of RPS3 in GLI2ΔN/YKNK-12 cells decreased the invasion of cells by 50% relative to that of control siRNA-transfected YKNK cells. Forced expression of RPS3 did not completely restore invasion by GLI2 knockdown. Our findings suggest that other factors are involved in GLI2-mediated invasion of osteosarcoma cells. Although the detailed molecular mechanisms of RPS3 expression by GLI2 have not been clarified, our present results showed that *RPS3* is a downstream gene of GLI2 and a novel mediator of osteosarcoma invasion. Wan et al. reported that RPS3 is a subunit of NF-κB and that it interacts with p65 [34]. Several reports showed that NF-κB promotes osteosarcoma cell invasion and metastasis [47–49]. These findings suggest that the GLI–RPS3–NF-κB pathway might promote the invasion of osteosarcoma cells. Furthermore, we previously reported that the Notch pathway is activated in osteosarcoma and is related to its growth [50]. It is known that NF-κB is an essential downstream regulator of the Notch pathway. Hence, RPS3 may be a regulatory molecule between the Hedgehog and Notch pathways in osteosarcoma.

It has been reported that the production of several ribosomal proteins is upregulated in several cancers [51]. Several oncogenes and tumor suppressors regulate the production of ribosomes [52–56]. In addition, RPS3 is involved in radioresistance or invasion of tumor cells [15,17]. We also showed that high expression levels of RPS3 as well as GLI2 in primary osteosarcoma tissue were correlated with poor clinical outcomes. However, further studies are required to elucidate the relationship between GLI2/RPS3 expression and prognosis, as the sample number was small in the current study. A recent study showed that ΔNP63α, a splice variant of p63, induces the expression of GLI2 and is involved in the malignant phenotype of osteosarcoma [44].Thus, the ΔNP63α–GLI2–RPS3 axis might have an important role in the progression of osteosarcoma. Kim et al. reported that the level of secreted RPS3 protein increases in malignant cells [57]. Thus, quantitation of RPS3 in serum may be a marker to diagnose primary or recurrent metastasis of osteosarcoma.

Taken together, we have shown that *RPS3* is a novel downstream gene of GLI2 that mediates osteosarcoma invasion and metastasis of osteosarcoma. These findings will improve the understanding of osteosarcoma pathogenesis, and indicate that the GLI2–RPS3 pathway may be an attractive therapeutic target for treating osteosarcoma metastasis.

Funding

This work was supported by Grants-in-Aid for Scientific Research (KAKENHI) (C) 19591725, (C) 20591786, (C) 21591919, (C) 21591920, (C) 22591663, and (C) 23592195, a Grant-in-Aid from the Ministry of Health, Labour and Welfare of Japan for the Third Term Comprehensive Control Research for Cancer, and Scientific Research on Priority Areas 201201976 to H. Nagao from the Grants-in-Aid for JSPS Fellows.

Acknowledgements

We are grateful to Hui Gao for her excellent technical assistance. We wish to thank the joint research laboratory of Kagoshima University Graduate School of Medical and Dental Sciences. Nagao-Kitamoto H., Setoguchi T., Kitamoto S., Nagano S., and Komiya S. conceived and designed the experiments. Nagao-Kitamoto H., Kitamoto S., Nakamura S., Tsuru A., Nagata M., Kitajima S., and Yonezawa S. performed the experiments. Ishidou Y., Yamamoto T., Maeda S., Setoguchi T., and Komiya S. analyzed the data. Yoshioka T. and Yokouchi M. contributed reagents/materials/analysis tools. Nagao-Kitamoto H. and Setoguchi T drafted the manuscript.

Conflict of interest

The authors have no conflicts of interest to disclose.

Appendix: Supplementary material

Supplementary data to this article can be found online at doi:10.1016/j.canlet.2014.10.042.

References

[1] M. Hegyi, A.F. Semsei, Z. Jakab, I. Antal, J. Kiss, M. Szendroi, et al., Good prognosis of localized osteosarcoma in young patients treated with limb-salvage surgery and chemotherapy, Pediatr. Blood Cancer 57 (2011) 415–422.
[2] S.M. Botter, D. Neri, B. Fuchs, Recent advances in osteosarcoma, Curr. Opin. Pharmacol. 16C (2014) 15–23.
[3] D.C. Allison, S.C. Carney, E.R. Ahlmann, A. Hendifar, S. Chawla, A. Fedenko, et al., A meta-analysis of osteosarcoma outcomes in the modern medical era, Sarcoma 2012 (2012) 704872.
[4] B.J. Miller, P. Cram, C.F. Lynch, J.A. Buckwalter, Risk factors for metastatic disease at presentation with osteosarcoma: an analysis of the SEER database, J. Bone Joint Surg. Am. 95 (2013) e89.
[5] L. Kager, A. Zoubek, U. Potschger, U. Kastner, S. Flege, B. Kempf-Bielack, et al., Primary metastatic osteosarcoma: presentation and outcome of patients treated on neoadjuvant Cooperative Osteosarcoma Study Group protocols, J. Clin. Oncol. 21 (2003) 2011–2018.
[6] V. Mialou, T. Philip, C. Kalifa, D. Perol, J.C. Gentet, P. Marec-Berard, et al., Metastatic osteosarcoma at diagnosis: prognostic factors and long-term outcome – the French pediatric experience, Cancer 104 (2005) 1100–1109.
[7] J.C. Clark, C.R. Dass, P.F. Choong, A review of clinical and molecular prognostic factors in osteosarcoma, J. Cancer Res. Clin. Oncol. 134 (2008) 281–297.
[8] M.U. Jawad, M.C. Cheung, J. Clarke, L.G. Koniaris, S.P. Scully, Osteosarcoma: improvement in survival limited to high-grade patients only, J. Cancer Res. Clin. Oncol. 137 (2011) 597–607.
[9] T. Ozaki, S. Flege, M. Kevric, N. Lindner, R. Maas, G. Delling, et al., Osteosarcoma of the pelvis: experience of the Cooperative Osteosarcoma Study Group, J. Clin. Oncol. 21 (2003) 334–341.
[10] K. Nybakken, N. Perrimon, Hedgehog signal transduction: recent findings, Curr. Opin. Genet. Dev. 12 (2002) 503–511.
[11] I. Caro, J.A. Low, The role of the hedgehog signaling pathway in the development of basal cell carcinoma and opportunities for treatment, Clin. Cancer Res. 16 (2010) 3335–3339.
[12] S.J. Scales, F.J. de Sauvage, Mechanisms of Hedgehog pathway activation in cancer and implications for therapy, Trends Pharmacol. Sci. 30 (2009) 303–312.
[13] S.S. Karhadkar, G.S. Bova, N. Abdallah, S. Dhara, D. Gardner, A. Maitra, et al., Hedgehog signalling in prostate regeneration, neoplasia and metastasis, Nature 431 (2004) 707–712.
[14] N. Kawabata, K. Ijiri, Y. Ishidou, T. Yamamoto, H. Nagao, S. Nagano, et al., Pharmacological inhibition of the Hedgehog pathway prevents human rhabdomyosarcoma cell growth, Int. J. Oncol. 39 (2011) 899–906.
[15] M. Kool, J. Koster, J. Bunt, N.E. Hasselt, A. Lakeman, P. van Sluis, et al., Integrated genomics identifies five medulloblastoma subtypes with distinct genetic profiles, pathway signatures and clinicopathological features, PLoS ONE 3 (2008) e3088.
[16] M. Souzaki, M. Kubo, M. Kai, C. Kameda, H. Tanaka, T. Taguchi, et al., Hedgehog signaling pathway mediates the progression of non-invasive breast cancer to invasive breast cancer, Cancer Sci. 102 (2011) 373–381.
[17] Y. Kim, J.W. Yoon, X. Xiao, N.M. Dean, B.P. Monia, E.G. Marcusson, Selective down-regulation of glioma-associated oncogene 2 inhibits the proliferation of hepatocellular carcinoma cells, Cancer Res. 67 (2007) 3583–3593.
[18] S. Thiyagarajan, N. Bhatia, S. Reagan-Shaw, D. Cozma, A. Thomas-Tikhonenko, N. Ahmad, et al., Role of GLI2 transcription factor in growth and tumorigenicity of prostate cells, Cancer Res. 67 (2007) 10642–10646.
[19] W. Yang, X. Liu, E. Choy, H. Mankin, F.J. Hornicek, Z. Duan, Targeting hedgehog-GLI-2 pathway in osteosarcoma, J. Orthop. Res. (2012).
[20] H. Nagao, K. Ijiri, M. Hirotsu, Y. Ishidou, T. Yamamoto, S. Nagano, et al., Role of GLI2 in the growth of human osteosarcoma, J. Pathol. 224 (2011) 169–179.
[21] S. Nakamura, S. Nagano, H. Nagao, Y. Ishidou, M. Yokouchi, M. Abematsu, et al., Arsenic trioxide prevents osteosarcoma growth by inhibition of GLI transcription via DNA damage accumulation, PLoS ONE 8 (2013) e69466.
[22] H. Nagao-Kitamoto, M. Nagata, S. Nagano, S. Kitamoto, Y. Ishidou, T. Yamamoto, et al., GLI2 is a novel therapeutic target for metastasis of osteosarcoma, Int. J. Cancer (2014).
[23] T. Schafer, B. Maco, E. Petfalski, D. Tollervey, B. Bottcher, U. Aebi, et al., Hrr25-dependent phosphorylation state regulates organization of the pre-40S subunit, Nature 441 (2006) 651–655.
[24] V. Hegde, M. Wang, W.A. Deutsch, Human ribosomal protein S3 interacts with DNA base excision repair proteins hAPE/Ref-1 and hOGG1, Biochemistry 43 (2004) 14211–14217.
[25] C.Y. Jang, J.Y. Lee, J. Kim, RpS3, a DNA repair endonuclease and ribosomal protein, is involved in apoptosis, FEBS Lett. 560 (2004) 81–85.
[26] J. Kim, L.S. Chubatsu, A. Admon, J. Stahl, R. Fellous, S. Linn, Implication of mammalian ribosomal protein S3 in the processing of DNA damage, J. Biol. Chem. 270 (1995) 13620–13629.
[27] S.H. Kim, J.Y. Lee, J. Kim, Characterization of a wide range base-damage-endonuclease activity of mammalian rpS3, Biochem. Biophys. Res. Commun. 328 (2005) 962–967.
[28] T.S. Kim, H.D. Kim, J. Kim, PKCdelta-dependent functional switch of rpS3 between translation and DNA repair, Biochim. Biophys. Acta 1793 (2009) 395–405.
[29] Y. Kim, H.D. Kim, J. Kim, Cytoplasmic ribosomal protein S3 (rpS3) plays a pivotal role in mitochondrial DNA damage surveillance, Biochim. Biophys. Acta 2013 (1833) 2943–2952.
[30] N. Sen, B.D. Paul, M.M. Gadalla, A.K. Mustafa, T. Sen, R. Xu, et al., Hydrogen sulfide-linked sulfhydration of NF-kappaB mediates its antiapoptotic actions, Mol. Cell 45 (2012) 13–24.
[31] Y.J. Joo, J.H. Kim, U.B. Kang, M.H. Yu, J. Kim, Gcn4p-mediated transcriptional repression of ribosomal protein genes under amino-acid starvation, EMBO J. 30 (2011) 859–872.
[32] H.D. Kim, T.S. Kim, J. Kim, Aberrant ribosome biogenesis activates c-Myc and ASK1 pathways resulting in p53-dependent G1 arrest, Oncogene 30 (2011) 3317–3327.
[33] S.H. Kim, J. Kim, Reduction of invasion in human fibrosarcoma cells by ribosomal protein S3 in conjunction with Nm23-H1 and ERK, Biochim. Biophys. Acta 1763 (2006) 823–832.
[34] F. Wan, D.E. Anderson, R.A. Barnitz, A. Snow, N. Bidere, L. Zheng, et al., Ribosomal protein S3: a KH domain subunit in NF-kappaB complexes that mediates selective gene regulation, Cell 131 (2007) 927–939.
[35] E.M. Wier, J. Neighoff, X. Sun, K. Fu, F. Wan, Identification of an N-terminal truncation of the NF-kappaB p65 subunit that specifically modulates ribosomal protein S3-dependent NF-kappaB gene expression, J. Biol. Chem. 287 (2012) 43019–43029.
[36] S. Yadavilli, L.D. Mayo, M. Higgins, S. Lain, V. Hegde, W.A. Deutsch, Ribosomal protein S3: a multi-functional protein that interacts with both p53 and MDM2 through its KH domain, DNA Repair (Amst) 8 (2009) 1215–1224.
[37] H. Nakahara, H. Misawa, T. Hayashi, E. Kondo, T. Yuasa, Y. Kubota, et al., Bone repair by transplantation of hTERT-immortalized human mesenchymal stem cells in mice, Transplantation 88 (2009) 346–353.
[38] D. Mokhtari, A. Barbu, I. Mehmeti, C. Vercamer, N. Welsh, Overexpression of the nuclear factor-kappaB subunit c-Rel protects against human islet cell death in vitro, Am. J. Physiol. Endocrinol. Metab. 297 (2009) E1067–E1077.
[39] M. Hirotsu, T. Setoguchi, H. Sasaki, Y. Matsunoshita, H. Gao, H. Nagao, et al., Smoothened as a new therapeutic target for human osteosarcoma, Mol. Cancer 9 (2010) 5.
[40] H. Nagao, T. Setoguchi, S. Kitamoto, Y. Ishidou, S. Nagano, M. Yokouchi, et al., RBPJ is a novel target for rhabdomyosarcoma therapy, PLoS ONE 7 (2012) e39268.
[41] M. Hu, J. Yao, D.K. Carroll, S. Weremowicz, H. Chen, D. Carrasco, et al., Regulation of in situ to invasive breast carcinoma transition, Cancer Cell 13 (2008) 394–406.
[42] Y. Matsunoshita, K. Ijiri, Y. Ishidou, S. Nagano, T. Yamamoto, H. Nagao, et al., Suppression of osteosarcoma cell invasion by chemotherapy is mediated by urokinase plasminogen activator activity via up-regulation of EGR1, PLoS ONE 6 (2011) e16234.
[43] S.U. Lauvrak, E. Munthe, S.H. Kresse, E.W. Stratford, H.M. Namlos, L.A. Meza-Zepeda, et al., Functional characterisation of osteosarcoma cell lines and identification of mRNAs and miRNAs associated with aggressive cancer phenotypes, Br. J. Cancer 109 (2013) 2228–2236.
[44] R.M. Ram Kumar, M.M. Betz, B. Robl, W. Born, B. Fuchs, DeltaNp63alpha enhances the oncogenic phenotype of osteosarcoma cells by inducing the expression of GLI2, BMC Cancer 14 (2014) 559.
[45] W.W. Lo, J.S. Wunder, B.C. Dickson, V. Campbell, K. McGovern, B.A. Alman, et al., Involvement and targeted intervention of dysregulated Hedgehog signaling in osteosarcoma, Cancer 120 (2014) 537–547.
[46] A.B. Mohseny, Y. Cai, M. Kuijjer, W. Xiao, B. van den Akker, C.E. de Andrea, et al., The activities of Smad and Gli mediated signalling pathways in high-grade conventional osteosarcoma, Eur. J. Cancer 48 (2012) 3429–3438.
[47] G. Berge, S. Pettersen, I. Grotterod, I.J. Bettum, K. Boye, G.M. Maelandsmo, Osteopontin – an important downstream effector of S100A4-mediated invasion and metastasis, Int. J. Cancer 129 (2011) 780–790.
[48] Z.L. Liu, J.H. Mao, A.F. Peng, Q.S. Yin, Y. Zhou, X.H. Long, et al., Inhibition of fatty acid synthase suppresses osteosarcoma cell invasion and migration via downregulation of the PI3K/Akt signaling pathway in vitro, Mol. Med. Rep. 7 (2013) 608–612.
[49] Z. Zhao, M.S. Wu, C. Zou, Q. Tang, J. Lu, D. Liu, et al., Downregulation of MCT1 inhibits tumor growth, metastasis and enhances chemotherapeutic efficacy in osteosarcoma through regulation of the NF-kappaB pathway, Cancer Lett. 342 (2014) 150–158.
[50] M. Tanaka, T. Setoguchi, M. Hirotsu, H. Gao, H. Sasaki, Y. Matsunoshita, et al., Inhibition of Notch pathway prevents osteosarcoma growth by cell cycle regulation, Br. J. Cancer 100 (2009) 1957–1965.
[51] D. Ruggero, P.P. Pandolfi, Does the ribosome translate cancer?, Nat. Rev. Cancer 3 (2003) 179–192.
[52] Y. Brandenburger, A. Jenkins, D.J. Autelitano, R.D. Hannan, Increased expression of UBF is a critical determinant for rRNA synthesis and hypertrophic growth of cardiac myocytes, FASEB J. 15 (2001) 2051–2053.
[53] A.H. Cavanaugh, W.M. Hempel, L.J. Taylor, V. Rogalsky, G. Todorov, L.I. Rothblum, Activity of RNA polymerase I transcription factor UBF blocked by Rb gene product, Nature 374 (1995) 177–180.
[54] L. Montanaro, D. Trere, M. Derenzini, Changes in ribosome biogenesis may induce cancer by down-regulating the cell tumor suppressor potential, Biochim. Biophys. Acta 2012 (1825) 101–110.
[55] D. Trere, C. Ceccarelli, L. Montanaro, E. Tosti, M. Derenzini, Nucleolar size and activity are related to pRb and p53 status in human breast cancer, J. Histochem. Cytochem. 52 (2004) 1601–1607.
[56] J. van Riggelen, A. Yetil, D.W. Felsher, MYC as a regulator of ribosome biogenesis and protein synthesis, Nat. Rev. Cancer 10 (2010) 301–309.
[57] Y. Kim, H.D. Kim, B. Youn, Y.G. Park, J. Kim, Ribosomal protein S3 is secreted as a homodimer in cancer cells, Biochem. Biophys. Res. Commun. 441 (2013) 805–808.

Metastatic bone tumors: Analysis of factors affecting prognosis and efficacy of CT and ^{18}F-FDG PET-CT in identifying primary lesions

HIROFUMI SHIMADA[1], TAKAO SETOGUCHI[2], MASAHIRO YOKOUCHI[1], HIROMI SASAKI[1], YASUHIRO ISHIDOU[3], ICHIRO KAWAMURA[1], MASAHIKO ABEMATSU[2], SATOSHI NAGANO[1] and SETSURO KOMIYA[1]

[1]Department of Orthopaedic Surgery; [2]The Near-Future Locomotor Organ Medicine Creation Course (Kusunoki Kai); [3]Department of Medical Joint Materials, Graduate School of Medical and Dental Sciences, Kagoshima University, Kagoshima 890-8520, Japan

Received April 28, 2014; Accepted May 28, 2014

DOI: 10.3892/mco.2014.326

Abstract. We analyzed the prognostic factors in patients with metastatic bone tumors and evaluated the efficacy of different modalities in identifying the primary lesions. A total of 145 patients with bone metastases who attended the orthopaedic outpatient clinic were included in this study. The most frequent site of bone metastases was the spine. The primary tumor type was differently distributed between patients with a known primary tumor at the first visit and those with an unknown primary lesion. The number of breast cancer cases was statistically significantly lower in the primary-unknown group. However, the number of myeloma cases was significantly higher in the primary-unknown group. Survival was significantly lower in the skeletal-related events (SREs) compared to that in the non-SREs group. Furthermore, survival was significantly worse in patients with a performance status (PS) of ≥2 compared to those with a PS of ≤1 and neurological complications occurred statistically more often in the group with worse PS (≥2). Survival rates were significantly lower in the non-spinal compared to those in the spinal metastatic group. Since the majority of breast cancer patients presented with metastasis in the spine, a breast cancer origin was a positive prognostic factor in patients with spinal metastases. Although there were no significant differences between computed tomography (CT) and ^{18}F-fluoro-2-deoxyglucose (^{18}F-FDG) positron emission tomography (PET)-CT in detecting primary lesions, CT may be the first choice due to its feasibility. In conclusion, lung cancer, SREs and worse PS were adverse prognostic factors for patients with bone metastasis. In addition, CT scans may be more useful for determining the primary lesion of a bone metastasis compared to ^{18}F-FDG PET-CT in a timelier manner.

Correspondence to: Dr Satoshi Nagano, Department of Orthopaedic Surgery, Graduate School of Medical and Dental Sciences, Kagoshima University, 8-35-1 Sakuragaoka, Kagoshima 890-8520, Japan
E-mail: naga@m2.kufm.kagoshima-u.ac.jp

Key words: metastatic bone tumor, skeletal-related events, performance status, prognostic factor, ^{18}F-fluoro-2-deoxyglucose positron emission tomography-computed tomography

Introduction

The recent advances in cancer treatment have improved patient survival. Cancers that have metastasized to the bones are considered to be at an advanced stage. Metastatic bone tumors often promote skeletal-related events (SREs), which include pathological fractures, neurological complications caused by compression of the spinal cord or cauda equina, or hypercalcemia, as well as the need for radiotherapy or surgery of the bone metastasis (1,2). Although the prognosis of patients with certain types of cancer has improved with the recent advances in chemotherapy and radiotherapy, patients with metastatic bone tumors require treatment of the primary lesion as well as anti-SRE assessment, in order to improve their quality of life and prognosis.

Metastatic bone tumors are treated by multidisciplinary teams, in which orthopaedic surgeons play an important role in the diagnosis and treatment of the bone metastasis, as well as in the detection of the primary cancer lesion. A delay in the diagnosis increases the risk of SREs and negatively affects the prognosis. In this regard, we investigated the background of patients with bone metastasis and the factors associated with prognosis. We investigated 145 cases of metastatic bone tumors with respect to the primary lesion, affected bone site and frequency of SREs and evaluated the effectiveness of a single computed tomography (CT) scan of the chest/abdomen/pelvis against that of ^{18}F-fluoro-2-deoxyglucose (^{18}F-FDG) positron emission tomography (PET)-CT scan in detecting the primary lesion of a metastatic bone tumor.

Materials and methods

Patients. In this retrospective study, we reviewed the medical records and imaging results of 145 patients with metastatic bone

tumors who were referred to the Department of Orthopaedic Surgery, Kagoshima University, between 2006 and 2011. The patients included 81 men and 64 women, with a mean age of 65 years (range, 29-87 years) and a mean follow-up of 9 months. A bone scan was performed on 97 patients.

The study protocol was approved by the Ethics Committee on Clinical Research at the Kagoshima University Hospital and all the patients provided written informed consent prior to inclusion.

Evaluation of imaging modalities and patient survival. Two well-trained radiologists reviewed all the bone scan results and compared them with radiographs, CT or magnetic resonance imaging (MRI) scans. The results of the imaging modalities were assessed taking into account clinical symptoms and any positive findings that indicated bone metastasis. To identify the primary lesion, a single chest/abdominal/pelvic CT, ^{18}F-FDG PET-CT and Tl scan were performed on each patient. Following an initial detection of the primary lesion, roentgenogram, MRI, biopsy and formal clinical follow-up were performed to obtain a definitive diagnosis. We examined the frequency of each primary tumor, bone metastatic site and incidence of SREs; we also estimated the survival rate and the detection rate of the original lesion using clinical examinations and evaluated the factors affecting survival. The survival rate was analyzed according to the Kaplan-Meier method. The clinical examinations that were performed to locate the original tumor were also evaluated.

Statistical analysis. Statistical analysis was performed using the Student's t-test or the Chi-square test and analyzed using Microsoft Office Excel software (Microsoft, Redmond, WA, USA). Kaplan-Meier analysis was performed using Kaplan 97 software. $P<0.05$ was considered to indicate statistically significant differences.

Results

Primary lesion and bone metastatic site. We examined the origin of all metastatic bone tumors (145 cases). The most frequent origin of bone metastasis was lung cancer (34 cases, 23%), followed by breast cancer (19 cases, 13%), kidney cancer (10 cases, 7%), liver cancer (10 cases, 7%), thyroid cancer (9 cases, 6%), prostate cancer (9 cases, 6%), colorectal cancer (8 cases, 6%), malignant lymphoma (7 cases, 5%), multiple myeloma (6 cases, 4%), gastric cancer (6 cases, 4%), and bladder cancer (4 cases, 3%) , as previously reported (3-5). The primary tumor could not be identified in 5 cases (3%; Fig. 1A). The Kaplan-Meier analysis demonstrated that the 1-, 2- and 3-year survival rate was 49, 34 and 18%, respectively, among all patients with bone metastasis (Fig. 2).

The most frequent bone metastatic site was the spine (143 cases), including the cervical vertebrae (28 sites), thoracic vertebrae (45 sites), lumbar vertebrae (53 sites) and sacrum (17 sites). Other sites of metastasis included the femur (28 cases), pelvis (27 cases), humerus (16 cases) and ribs (15 cases) (Fig. 1B). Our findings revealed that the most frequent spinal metastatic site was the lumbar spine, followed by the thoracic and cervical spine. It was previously reported that the most frequent metastatic site was the thoracic spine, followed by the lumbar and cervical spine (6-9). To explain this discrepancy, we compared the primary malignant tumor between the lumbar and thoracic metastatic groups. We identified no statistically significant difference in the primary lesion between these two groups.

The primary tumor site distribution was compared between patients with a known primary lesion and those with unknown primary lesion at the first visit. In the primary-known group (n=84), the primary tumors were breast (18 cases, 21%), lung (11 cases, 13%), liver (9 cases, 11%), thyroid (7 cases, 8%) and kidney cancer (6 cases, 7%). In the primary-unknown group (n=61), the primary tumors were lung cancer (23 cases, 38%), myeloma (5 cases, 8%), kidney and prostate cancer and malignant lymphoma (4 cases each, 7%) (Table I). During the follow-up period, the primary lesion was not identified in 5 cases. The number of breast cancer cases was statistically significantly lower in the primary-unknown group. However, the number of myeloma was significantly higher in the primary-unknown group.

Factors affecting the prognosis of bone metastasis. We first investigated the association between prognosis and SREs and observed that survival was significantly lower in the SREs compared to that in the non-SREs group (Fig. 3A). In addition, PS was found to be an important factor for the selection of the appropriate chemotherapeutic regimen and, therefore, we investigated the association between patient prognosis and PS (10,11) and survival was found to be significantly lower in the PS≥2 compared to that in the PS≤1 group (Fig. 3B). Since the most frequent bone metastatic site was the spine, we investigated the association between spinal metastasis and patient prognosis. The Kaplan-Meier analysis revealed that the 1- and 3-year survival rates for patients with spinal metastases was 56 and 23%, respectively. Furthermore, the 1- and 3-year survival rates for patients with non-spinal metastases were 37 and 8%, respectively. Therefore, survival rates were significantly lower in the non-spinal compared to those in the spinal metastatic group (Fig. 3C). To determine which factors were associated with a favorable prognosis in patients with spinal metastasis, we investigated the association between prognosis and neurological complications caused by compression of the spinal cord or cauda equina. The Kaplan-Meier analysis revealed that neurological complications did not exert a significant effect on survival for any of the patients with bone metastasis (Fig. 3D). We next investigated the primary lesion in the non-spinal and spinal metastatic groups and found that the number of breast cancer patients was higher in the spinal metastatic group (Table II).

Association between SREs and prognosis or PS. We demonstrated that the survival rate was significantly lower in the PS≥2 compared to that in the PS≤1 group (Fig. 3B). We investigated the association between SREs and PS. The incidence of SREs among all the bone metastatic cases was 107 (74%). Hypercalcemia (serum calcium levels, 10.4-12.6 mg/dl; normal range, 8.5-10.3 mg/dl) occurred in 8 cases (5.5%) and was accompanied by renal dysfunction in 4 of the 8 cases (Table IIIA). Symptoms caused by compression of the spinal cord or cauda equina were observed in 36 cases (24.8%), including symptoms of the cervical (11 cases), thoracic (15 cases) and lumbar segments (10 cases) (Table IIIA and B).

Table I. Comparison of the primary tumor site between groups with known and unknown origin at initial visit.

Origin known at initial visit	Cases (%)	Origin unknown → diagnosed	Cases (%)
Breast	18[a] (21)	Lung	23 (38)
Lung	11 (13)	Myeloma	5[b] (8)
Liver	9 (11)	Kidney	4 (7)
Thyroid	7 (8)	Prostate	4 (7)
Kidney	6 (7)	Lymphoma	4 (7)
Prostate	5 (6)	Gastric	3 (5)
Colorectal	5 (6)	Colorectal	3 (5)
Lymphoma	3 (4)	Thyroid	2 (3)
Esophagus	3 (4)	Pancreas	2 (3)
Gastric	3 (4)	Bladder	2 (3)
Uterus	3 (4)	Breast	1[a] (2)
Tongue	2 (2)	Others	8 (12)
Bladder	2 (2)		
Myeloma	1[b] (1)		
Others	6 (7)		
Total	84 (100)	Total	61 (100)

[a]P<0.01, [b]P<0.05.

Table II. Comparison of the primary tumor site between groups with and without spinal metastasis.

Spinal metastasis (+)	Cases	Spinal metastasis (-)	Cases
Lung	22	Lung	12
Breast	17[a]	Kidney	5
Liver	8	Thyroid	4
Prostate	7	Liver	4
Colorectal	6	Bladder	4
Thyroid	5	Lymphoma	3
Kidney	5	Esophagus	2
Myeloma	5	Gastric	2
Gastric	4	Breast	2[a]
Lymphoma	4	Prostate	2
Pancreas	3	Colorectal	2
Tongue	2	Others	4
Others	11		
Total	99	Total	46

[a]P<0.05.

Pathological fractures were detected in 23 cases (15.9%), including fractures of the extremities (femur, 9 cases; and humerus, 5 cases); thoracic vertebrae, 3 cases; and lumbar vertebrae, 2 cases (Table IIIC). Surgery for SREs was performed in 26 cases (18%), including internal fixation (10 cases), resection plus reconstruction (9 cases), spinal decompression (2 cases), spinal fusion (4 cases) and total en bloc spondylectomy (1 case)

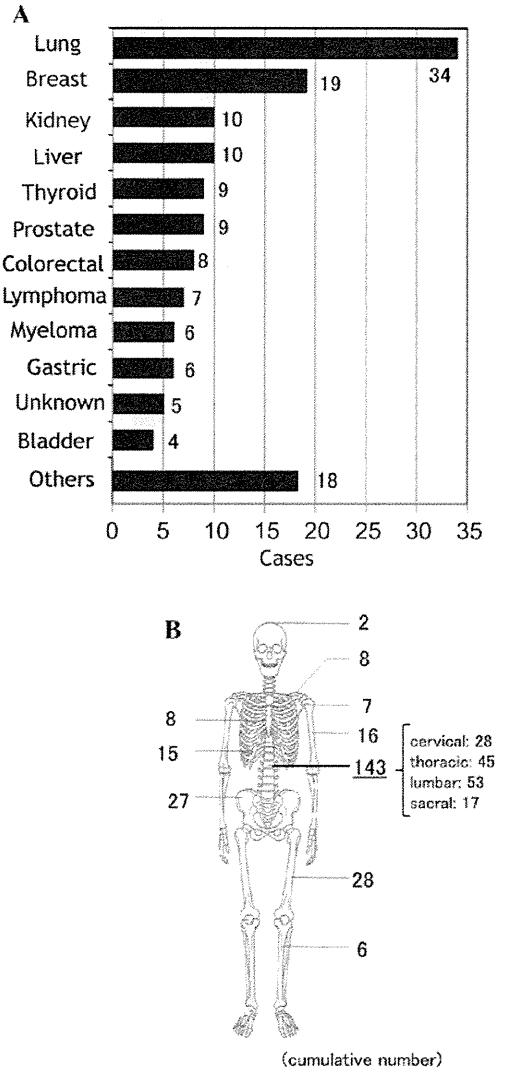

Figure 1. Number of bone metastases. (A) Number of cases with bone metastases per primary lesion. (B) Number of patients per bone metastatic site.

(Table IIID). Radiotherapy for bone metastasis was performed in 75 cases (51.7%).

In the group with better PS scores (≤1, n=32), pathological fractures were detected in 3 cases (9.4%), neurological complications were observed in 3 cases (9.4%), hypercalcemia occurred in 2 cases (6.3%), surgery for SREs was performed in 4 cases (12.5%) and radiotherapy was performed in 14 cases (43.8%). In the group with poor PS scores (≥2, n=113), pathological fractures were detected in 20 cases (17.7%), neurological complications caused by compression of the spinal cord or cauda equina were observed in 33 cases (29.2%), hypercalcemia occurred in 6 cases (5.3%), surgery for SREs was performed in 24 cases (21.2%) and radiotherapy was performed in 70 cases (61.9%). Among the 5 SREs, only neurological complications were found to be significantly increased in the group with a PS score of ≥2 compared to that with a PS score of ≤1 (Table IIIE).

Identification of the primary lesion using imaging studies. The primary tumor site was identified using diagnostic imaging in

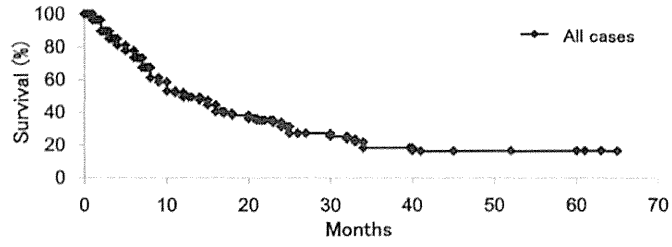

Figure 2. Overall survival rate. The Kaplan-Meier analysis revealed that the 1-, 2- and 3-year survival rates were 49, 34 and 18%, respectively, among all patients with bone metastasis.

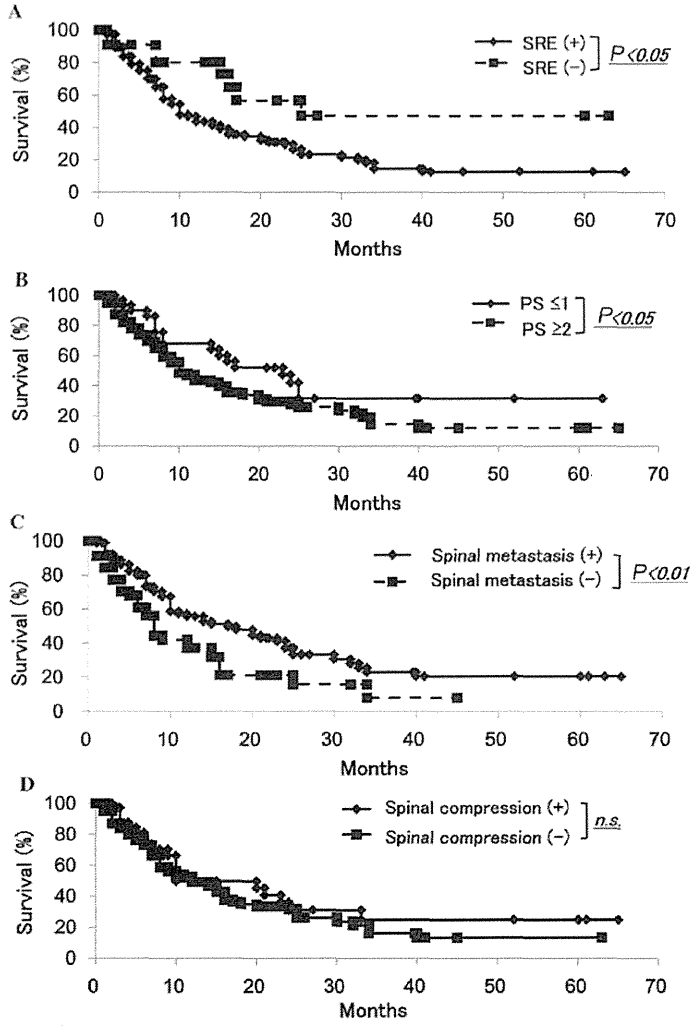

Figure 3. Comparison of survival rates. The Kaplan-Meier analysis revealed that (A) survival was significantly lower in the skeletal-related events (SREs) compared to that in the non-SREs group; (B) survival was significantly lower in the performance status (PS)≥2 compared to that in the PS≤1 group; (C) survival rates were significantly lower in the non-spinal compared to those in the spinal metastatic group; and (D) neurological complications did not exert a significant effect on survival for any bone metastatic patients; n.s., not signifigant.

49 cases, which included CT (32 cases) and ^{18}F-FDG PET-CT (17 cases) (Table IVA). Whole-body bone scans and Tl scans could not identify the primary lesion. CT was performed on 55 patients (90%) in whom the primary tumor was not identified during the first visit to the hospital. The time interval from the first visit until the CT scan was performed was 3.6 days. ^{18}F-FDG PET-CT was performed on 39 patients (64%) with unidentified primary tumors. The time interval from the first visit until the ^{18}F-FDG PET-CT was performed was 7.2 days. CT scans helped identify the following primary cancers: lung (16 cases), kidney (3 cases), thyroid (2 cases), pancreatic (2 cases) and bladder cancer (2 cases), myeloma (2 cases) and others (5 cases). ^{18}F-FDG PET-CT scans identified the following primary cancers: lung (6 cases), prostate (4 cases),

Table III. Analysis of SREs.

A, Number of cases per SRE

Cases	Fracture	Hyper-calcemia	Spinal compression	Radiation therapy for bone metastasis	Surgery for bone metastasis	Total cases with SREs
No. (%)	23 (15.9)	8 (5.5)	36 (24.8)	75 (51.7)	26 (17.9)	107 (73.8)

B, Distribution of spinal metastases in patients with symptoms caused by compression of spinal cord or cauda equina

Cases	Cervical spine	Thoracic spine	Lumbar spine	Total
No. (%)	11 (30.5)	15 (41.7)	10 (27.8)	36 (100)

C, Pathological fractures

Cases	Femur	Humerus	Thoracic spine	Lumbar spine	Others	Total
No. (%)	9 (39.1)	5 (21.7)	3 (13.0)	2 (8.7)	4 (17.5)	23 (100)

D, Type of surgery for pathological fractures

Cases	Resection plus reconstruction	Internal fixation	Spinal fusion	Spinal decompression	Total en bloc spondylectomy	Total
No. (%)	9 (34.6)	10 (38.5)	4 (15.4)	2 (7.7)	1 (3.8)	26 (100)

E, Incidence of SREs in groups with better (≤1) and worse (≥2) PS

Cases, no. (%)	Fracture	Hypercalcemia	Spinal compression	Radiation therapy for bone metastasis	Surgery for bone metastasis
PS≤1 (n=32)	3 (9.4)	2 (6.3)	3 (9.4)[a]	14 (43.8)	4 (12.5)
PS≥2 (n=113)	20 (17.7)	6 (5.3)	33 (29.2)[a]	70 (61.9)	24 (21.2)

SRE, skeletal-related event; PS, performance status. [a]P<0.05.

colorectum (2 cases) and others (5 cases) (Table IVB). A CT scan alone was able to identify primary tumors of the bladder (2 cases), myeloma (2 cases) and thyroid cancer (1 case) that could not be identified using ^{18}F-FDG PET-CT imaging. However, a ^{18}F-FDG PET-CT scan alone was able to identify primary lung cancer (1 case), myeloma (1 case) and colorectal cancer (1 case) (Table IVB). Although there were no significant differences between CT and ^{18}F-FDG PET-CT scans in the detection of primary lesions, CT scans were found to be more useful in determining the primary lesion of a bone metastasis in a timelier manner.

Discussion

Over the last few years, the number of cancer patients has increased. The majority of patients who are diagnosed with bone metastasis are referred to an orthopaedic surgeon to evaluate the bone metastasis and its progression, locate the primary lesion and decide upon treatment options.

We demonstrated that metastasis to the spine was the most frequent, followed by the femur and pelvic bone, as previously reported (6). Of the total bone metastases, the ratio of spinal metastasis was 54.7% (141/258 lesions). Our findings revealed that the number of bone metastases to the spine was lower compared to what was previously reported; in addition, the incidence of lumbar metastasis was relatively high compared to previous reports (6-9,12). Overall survival depends mainly on the type of the primary tumor. We did not identify a statistically significant difference regarding the type of primary tumor between the lumbar and thoracic metastatic groups. The relatively low number of spinal metastases may be the cause of this discrepancy. However, further studies are required to elucidate this issue.

It has been reported that the median overall survival of patients with spinal metastases is 7 months. In addition, only 10-20% of patients with spinal metastases remained alive at 2 years after diagnosis (12). We found that the 1-year survival rate was 49% and the 3-year survival rate was 18% among